Analysis of Average Torque in Switched Reluctance Motor with Unipolar and Bipolar Excitations Based on an Improved Fourier Series Model

X.Liu[1,2], Z.P.Pan[1], Z.Q.Zhu[2]
[1]College of Electrical Engineering, Zhejiang University, Hangzhou, China
[2]Department of Electronic and Electric Engineering, University of Sheffield, Sheffield, U.K.
E-mail: Elp09xll@sheffield.ac.uk, Panzaiping@zju.edu.cn, z.q.zhu@sheffield.ac.uk

***Abstract*-Switched reluctance machines (SRMs) are usually excited by unipolar current by employing asymmetric bridge inverters. It is also possible to excite SRMs by bipolar current using a three-phase bridge inverter. The main objective of this paper is to derive general analytical expression of average torque in SRMs under both unipolar and bipolar excitations, and to analyze their average torque under three working bipolar excitation patterns, with reference to unipolar excitation. All analyses are verified by the finite element analysis and measurements on a prototype 6/4 SRM.**

I. INTRODUCTION

Switched reluctance machines (SRM) have been applied to applications, ranging from domestic appliances to more-electric aircrafts, due to low cost, simple and robust rotor structure without any winding or permanent magnet. In general, SRMs are usually excited by unipolar current by employing asymmetric bridge inverters, Fig.1. It is also possible to excite SRMs by bipolar current using a three-phase bridge inverter [1][2][3], Fig.2. In [2] the experimental results of SRMs with bipolar current excitation are presented by using a more standard 3-phase bridge inverter. It shows that by applying bipolar excitation in SRMs a reduction in noise emission [2] and an increase in efficiency due to short flux path of magnetic circuit can be achieved [3]. However, the principle of torque production is not presented theoretically, and only one pattern of bipolar excitation is described. In this paper, from the theoretical analysis of torque production, the principle of SRMs excited by the bipolar current will be obtained, thus several new bipolar excitation patterns will be derived and analyzed theoretically.

In order to derive the operation principle of SRMs under both unipolar and bipolar excitations, it is necessary to model their electromagnetic torque. However, SRMs are usually designed to operate under deep magnetic saturation. Therefore, the nonlinear characteristic of self-inductance makes it difficult to model SRMs in order to accurately calculate the produced electromagnetic torque.

In modelling SRMs, several methods such as quasi-linear model[4][5], Ψ-i diagram [6], curve-fitting function to represent the flux-linkage against both current and rotor position[7] have been proposed. However, quasi-linear is not accurate, which makes it more suitable for qualitative analysis. Ψ-i diagram and curve fitting function require the stored data of nonlinear relationship of flux-linkage with both phase current and rotor position. Analytical method for determining the coefficients of Fourier series is also often used although it is usually simplified and may lead to big error due to heavy magnetic saturation. For example, one approach takes the first-order harmonic as the mean value of the maximum and minimum self-inductances [8]. Another approach is simply to account for the angle from the unaligned position to the beginning of overlap [9].

The main objective of this paper is to derive the general analytical expression of average torque in SRMs under unipolar and bipolar excitations, and to analyze their average torque under three working bipolar excitation patterns, with reference to unipolar excitation. Both finite element (FE) and analytical methods are employed in the analyses of average torque under alternate excitations. Analytical analyses are based on an improved Fourier series expression of winding inductance against the rotor position, with due account for the magnetic saturation. At last, the electromagnetic torque produced by the unipolar and three bipolar excitation patterns is verified by the FEA and measurements on a prototype 6/4 SRM, together with the analytical analysis.

II. FOURIER SERIES EXPRESSION OF VARIATION OF SELF-INDUCTANCE WITH ROTOR POSITION

Due to the symmetry, the accuracy of maximum and minimum inductances obtained by analytical method at both aligned and unaligned positions is higher than that at other positions. Therefore, it is preferable to model SRMs using the maximum and minimum self-inductances with due account for the magnetic saturation. Establishing the model just from the geometry and material property not only saves time and cost but also convenient to apply in the motor design routine.

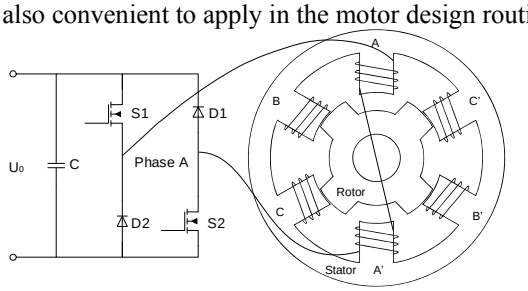

Fig.1 Three-phase 6/4 SRM and one phase leg of asymmetric bridge.

978-1-4244-8218-4/10/$26.00 ©2010 IEEE

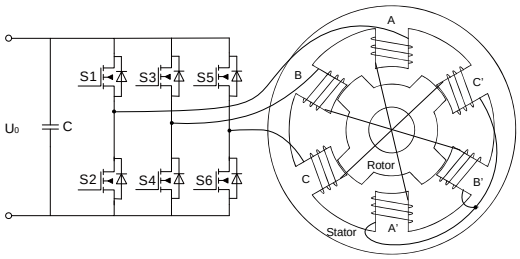

Fig.2 Three-phase 6/4 SRM and three-phase bridge inverter.

Because the mutual inductance is much smaller comparing with the self-inductance, it is reasonable to neglect the mutual inductance in SRMs [4][5][6]. To obtain the nonlinear model of SRMs, the self-inductance is divided into four regions, as shown in Fig.3, in which

$$L(\theta)=\begin{cases} L_u & 0<\theta\le\theta_1 \\ k\left\{\theta-[\frac{\pi}{N_r}-\frac{1}{2}(\beta_r'+\beta_s')]\right\}+L_u & \theta_1<\theta\le\theta_2 \\ L_a & \theta_2<\theta\le\theta_3 \\ -k\left\{\theta-[\frac{\pi}{N_r}+\frac{1}{2}(\beta_r'-\beta_s')]\right\}+L_a & \theta_3<\theta\le\theta_4 \\ L_u & \theta_4<\theta\le 2\pi/N_r \end{cases} \quad (1)$$

where L_u, L_a, N_r, β_s', β_r' stand for self-inductance at unaligned and aligned positions, rotor pole number, stator pole arc, rotor pole arc with due account for the local saturation, and the slop k can be expressed as $(L_a- L_u)/\beta_s$. It is usually very difficult to consider the local saturation since it is affected by the current excitation, the airgap length, and the machine geometries. However, some empirical methods are available and have been widely employed as good approximation [6]. By way of example, an adjusting angle is applied to stator and rotor pole arcs, which is equal to $3g/r_1$, where g and r_1 stand for the air gap length and the rotor outer radius. θ_1, θ_2, θ_3, θ_4 are determined by the stator and rotor pole arcs with due account for the local saturation which is written in (2).

$$\begin{bmatrix}\theta_1\\ \theta_2\\ \theta_3\\ \theta_4\end{bmatrix}=\begin{bmatrix}\pi/N_r-(\beta_r'+\beta_s')/2\\ \pi/N_r-(\beta_r'-\beta_s')/2\\ \pi/N_r+(\beta_r'-\beta_s')/2\\ \pi/N_r+(\beta_r'+\beta_s')/2\end{bmatrix} \quad (2)$$

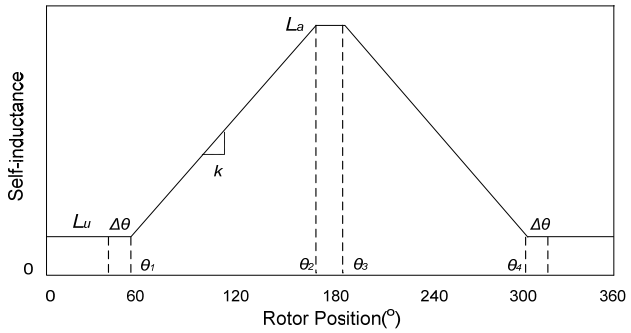

Fig.3 Variation of self-inductance with rotor position.

Due to the periodic property of self-inductance, it can be expressed by Fourier series expression, i.e.

$$L(\theta)=\frac{L_0}{2}+L_1\cos(N_r\theta)+L_2\cos(2N_r\theta)+\cdots \quad (3)$$

in which,

$$\begin{aligned} L_0&=\frac{N_r}{\pi}\int_0^{2\pi/N_r}L(\theta)d\theta \\ &=\frac{N_r}{\pi}\left\{\begin{aligned}&\int_0^{\theta_1}L_u d\theta+\int_{\theta_1}^{\theta_2}[k(\theta-\theta_1)+L_u]d\theta+\int_{\theta_2}^{\theta_3}L_a d\theta\\ &+\int_{\theta_3}^{\theta_4}[-k(\theta-\theta_3)+L_a]d\theta+\int_{\theta_4}^{2\pi/N_r}L_u d\theta\end{aligned}\right\} \\ &=\frac{L_a(i)N_r\beta_r'}{\pi}+\frac{L_u}{\pi}(2\pi-N_r\beta_r') \end{aligned} \quad (4)$$

$$\begin{aligned} L_n&=\frac{N_r}{\pi}\int_0^{2\pi/N_r}L(\theta)\cos(nN_r\theta)d\theta \\ &\frac{N_r}{\pi}\left\{\begin{aligned}&\int_0^{\theta_1}L_u\cos(nN_r\theta)d\theta+\int_{\theta_1}^{\theta_2}[k(\theta-\theta_1)+L_u]\cos(nN_r\theta)d\theta\\ &+\int_{\theta_2}^{\theta_3}L_a\cos(nN_r\theta)d\theta+\int_{\theta_3}^{\theta_4}[-k(\theta-\theta_3)+L_a]\cos(nN_r\theta)d\theta\\ &+\int_{\theta_4}^{2\pi/N_r}L_u\cos(nN_r\theta)d\theta\end{aligned}\right\} \\ &=(-1)^n\frac{4}{n^2\pi N_r\beta_s'}\sin(\frac{1}{2}nN_r\beta_r')\sin(\frac{1}{2}nN_r\beta_s')(L_a(i)-L_u) \end{aligned} \quad (5)$$

In the foregoing coefficients, except the self-inductance at aligned position L_a which is a function of phase current, the others are all constant. From Fig.4 it can be seen that at the current < I_s the self-inductance is almost constant, while at current > I_s the self-inductance reduces approximately with a constant slope. Therefore, by applying the piecewise linear function it can obtain good agreement with FEA results, which can be written as:

$$L_a=\begin{cases} L_m & i\le I_s \\ L_m+k_s(i-I_s) & i>I_s \end{cases} \quad (6)$$

where the slope k_s can be obtained by the data from the lumped parameter magnetic circuit, FEA, or experiments.

TABLE I. MAIN PARAMETERS OF PROTOTYPE SRM

Stator outer diameter	93.8mm	Stack length	46.9mm
Rotor diameter	46.9mm	Stator pole arc	30°
Air gap	0.3mm	Rotor pole arc	32°

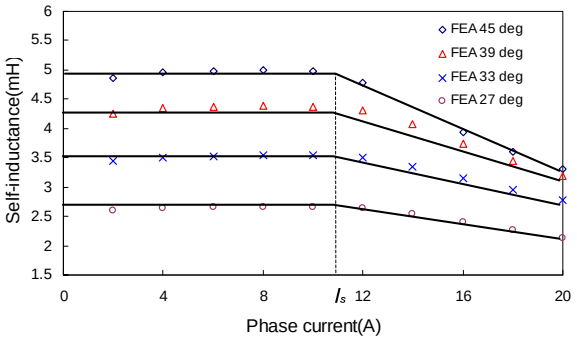

Fig.4 Self-inductance at aligned rotor position (45 deg) and other rotor positions.

In Fig.4 it can be seen that the saturation slope k_s is also a function of rotor position. Due to the assumption of unsaturation at unaligned position, the saturation slope can be determined by the overlap area of stator pole and rotor pole. To approximately model the relationship between the saturation slope and the rotor position, a piecewise linear function is applied, i.e.

$$k_s(\theta)=\begin{cases}0 & \\ \dfrac{K_s^a}{\beta_s}(\theta-\theta_1) & 0<\theta\le\theta_1\\ K_s^a & \theta_1<\theta\le\theta_2\\ -\dfrac{K_s^a}{\beta_s}(\theta-\theta_3)+K_s^a & \theta_2<\theta\le\theta_3\\ 0 & \theta_3<\theta\le\theta_4\\ & \theta_4<\theta\le 2\pi/N_r\end{cases} \tag{7}$$

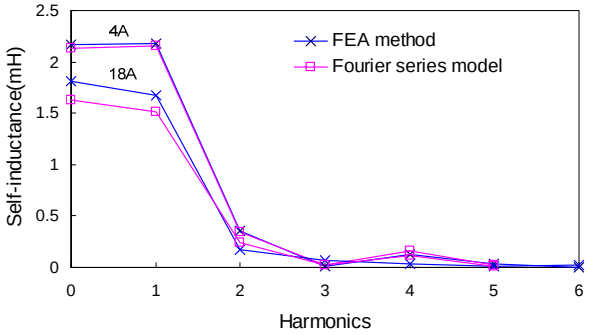

Fig.5 Comparison harmonics of self-inductance of one single phase in SRM.

where $K^a{}_s$ is the saturation slope at aligned position. Therefore, the saturation slope can also be expressed by the Fourier series with the coefficients as functions of rotor position. Therefore, the saturation slope k_s can be written as:

$$k_s(\theta)=b_0/2+b_1\cos(N_r\theta)+\cdots+b_n\cos(nN_r\theta) \tag{8}$$

where

$$\begin{aligned}b_0&=\frac{N_r}{\pi}\int_0^{2\pi/N_r}k_s(\theta)d\theta\\&=\frac{N_r}{\pi}\left[\begin{aligned}&\int_{\theta_1}^{\theta_2}\frac{K_s^a}{\beta_s}(\theta-\theta_1)d\theta+\int_{\theta_2}^{\theta_3}K_s^a d\theta\\&+\int_{\theta_2}^{\theta_3}-\frac{K_s^a}{\beta_s}(\theta-\theta_3)+K_s^a d\theta\end{aligned}\right]\\&=\frac{K_s^a N_r\beta_r'}{\pi}\end{aligned} \tag{9}$$

$$\begin{aligned}b_n&=\frac{N_r}{\pi}\int_0^{2\pi/N_r}k_s(\theta)\cos(nN_r\theta)d\theta\\&=\frac{N_r}{\pi}\left\{\begin{aligned}&\int_{\theta_1}^{\theta_2}\frac{K_s^a}{\beta_s}(\theta-\theta_1)\cos(nN_r\theta)d\theta+\int_{\theta_2}^{\theta_3}K_s^a\cos(nN_r\theta)d\theta\\&+\int_{\theta_2}^{\theta_3}\left[-\frac{K_s^a}{\beta_s}(\theta-\theta_3)+K_s^a\right]\cos(nN_r\theta)d\theta\end{aligned}\right\}\\&=(-1)^n\frac{4K_s^a}{n^2\pi N_r\beta_s'}\sin(\frac{1}{2}nN_r\beta_s')\sin(\frac{1}{2}nN_r\beta_r')\end{aligned} \tag{10}$$

Fig.5 compares the FEA predicted and Fourier series expression obtained harmonics at both unsaturation and saturation conditions.

III. Average Torque Calculation Under Conventional Unipolar Excitation Based on Fourier Series Model

In SRMs, the average torque of SRM is important since it can reveal the basic principle of torque production, and reflect the operation conditions. Due to periodic nature of phase current waveform, it can be expressed as a Fourier series with respect to the time t. i.e.

$$i=I_0+\sum_{n=1}^{\infty}I_n\cos\left(n\omega N_r(t+t_n)\right) \tag{11}$$

where ω, N_r stands for the mechanical rotor speed, and rotor pole number. The origin time ($t=0$) is at the instant when the rotor slot is aligned with the stator pole of phase A. In (11) the I_0 is the constant part and I_n and t_n are the amplitude and initial time of harmonics.

A. Unsaturation case

When the phase current is less than I_s at the knee point of saturation, illustrated in Fig.4 in Section II, the aligned self-inductance is almost constant. Therefore, the flux-linkage in this phase is in direct proportion to the current. Then, the torque production of one single phase can be derived as:

$$T=\frac{1}{2}i^2\frac{dL(\theta)}{d\theta} \tag{12}$$

Substitute the self-inductance and phase current, both of which are expressed as functions of rotor position and time, then the torque equation is:

$$T=-\frac{1}{2}(I_0+\sum_{n=1}^{\infty}I_n\cos(nN_r\omega(t+t_n))^2\cdot(\sum_{n=1}^{\infty}L_nN_rn\cdot\sin(nN_r\theta)) \tag{13}$$

where L_n is the n^{th} harmonic of self-inductance of SRM. It can be seen that the instantaneous torque is quite complicated in the above expression. However, there are a lot of items which are periodic functions, and they will make no contribution to the total average torque production. Therefore, the expression of average torque in SRMs can be obtained by the integration over one cycle, i.e.

$$\begin{aligned}\overline{T}&=\frac{N_r}{2\pi}\int_0^{2\pi/N_r}Td\theta\\&=\sum_{n=1}^{\infty}\frac{n}{2}N_rI_0I_nL_n\sin(\theta_n)+\sum_{n=1}^{\infty}\frac{n}{4}N_rI_n^2L_{2n}\sin(2\theta_n)\\&-\sum_{m=1}^{\infty}\sum_{n=1}^{\infty}\frac{m}{4}N_rI_nI_{n+m}L_m\sin(\theta_n-\theta_{n+m})\\&+\sum_{m=1}^{\infty}\sum_{n=1}^{\infty}\frac{2m+n}{4}N_rI_mI_{m+n}L_{n+2m}\sin(\theta_m+\theta_{n+2m})\end{aligned} \tag{14}$$

where $\theta_n=nN_r\omega t$, which means the leading angle of the n^{th} phase current harmonic with reference to the defined time origin.

In (14), the torque expression consists of four parts. The first part is produced by the constant current I_0, current harmonics I_n, the corresponding coefficient of self-inductance L_n, and the leading angle of phase current ahead of the reference θ_n. The second part in (14) is only produced by the single harmonic, the coefficient of self-inductance with twice current frequency, and twice leading angle of phase current ahead of self-inductance at the instant of aligned position. The third and fourth parts are constituted by the phase current of two different frequencies, the frequency of self-inductance coefficient equals to the difference and sum of frequencies of two different current harmonics, and the difference and sum of leading angles of two different current harmonics ahead of self-inductance at the instant of aligned position.

B. Saturation case

The expression (14) is derived at the assumption of unsaturation. However, to increase the torque density the

SRMs usually operate under saturation. The saturation case of SRM is not only related to the motor structure, but also the magnetic property of laminations. Therefore, it is usually quite difficult to obtain the nonlinear relationship of inductance against phase current.

However, based on the model which is presented in Section II the coefficients of self-inductance have already taken the magnetic saturation into consideration. Therefore, the torque expression under saturation can be written as:

$$T = -\frac{1}{2}(I_0 + \sum_{n=1}^{\infty} I_n \cos(nN_r\omega t + \theta_n))^2 N_r \sum_{n=1}^{\infty} nL_n \sin(nN_r\theta) + \begin{pmatrix} \frac{1}{3}(I_0 + \sum_{n=1}^{\infty} I_n \cos(nN_r\omega t + \theta_n))^3 + \frac{1}{6} I_s^3 \\ -\frac{1}{2} I_s (I_0 + \sum_{n=1}^{\infty} I_n \cos(nN_r\omega t + \theta_n))^2 \end{pmatrix} \frac{dk_s}{d\theta} \quad (15)$$

in which, k_s is the slope of saturation, which is determined by the overlap area of stator pole and rotor pole.

IV. Average Torque Calculation Under Bipolar Excitations Based on Fourier Series Model

In this section, the principle for torque production under new bipolar current excitations of using a 3-phase bridge inverter will be developed for the first time.

In (14) it has shown that the average torque can be divided into four parts. Except the first part, the other parts have nothing to do with direct current (DC) and are produced only by alternate currents (AC). Therefore, it is possible to drive SRM with bipolar excitation using a three-bridge inverter (Fig.2).

A. Driven by Current of Single Frequency

In (14), the second part is the torque which is only related to the AC excitations. However, in this part the minimum order of self-inductance is two, which leads to the contribution of this part to total torque production under unipolar excitation is not significant. In order to utilize this part to produce the dominate torque, the first order harmonic of self-inductance L_1 should be considered in this part. Therefore, the minimum frequency of AC excitations must equal to half of the frequency of ωN_r which can be written as:

$$i = \sum_{n=1}^{\infty} I_n \cos\left(\frac{n\omega N_r}{2}(t + t_n)\right) \quad (16)$$

Similar to the torque under unipolar excitation, at the amplitude of AC excitation less than I_s the torque equation can be obtained by substituting (16) into (12), and eliminating the periodic items by integrating over one cycle, the overall average torque can be expressed as:

$$\begin{aligned} \overline{T} = & \sum_{n=1}^{\infty} \frac{n}{8} I_n^2 L_n N_r \sin(2\theta_n) \\ & - \sum_{m=1}^{\infty}\sum_{n=1}^{\infty} \frac{m}{4} I_n I_{n+2m} L_m N_r \sin(\theta_n - \theta_{n+2m}) \\ & + \sum_{m=1}^{\infty}\sum_{n=1}^{\infty} \frac{m+n}{4} I_m I_{m+2n} L_{m+n} N_r \sin(\theta_m + \theta_{m+2n}) \end{aligned} \quad (17)$$

As expected, the first part in (17) contains the item which is contributed by the first order harmonic of self-inductance L_1. Due to the dominance of L_1 among all harmonics of self-inductance, the SRMs under this excitation will produce considerable average torque.

B. Driven by Current of Two-Frequencies-I

In (14), the third part only contains the alternate currents and the fundamental component of self-inductance. However, the minimal order of self-inductance in the fourth part is two, which means the overall torque production of this part is relatively small. Therefore, the contribution of the third part can be significant if appropriate currents are injected into the windings. In the case of m=n=1, the fundamental component of self-inductance is involved in this part, which will have a great contribution to the overall torque. In other words, the average torque can be produced by a combination of AC excitations having two different frequencies, such as the first and second order harmonics of phase current. Therefore, another AC excitation can be obtained, i.e.

$$i = \sum_{n=1}^{\infty} I_n \cos(nN_r\omega t + \theta_n) \quad (18)$$

Substitute (18) into (12), and eliminate the periodic items, the average torque production can be expressed as:

$$\begin{aligned} \overline{T} = & \sum_{n=1}^{\infty} \frac{n}{4} N_r I_n^2 L_{2n} \sin(2\theta_n) \\ & + \sum_{m=1}^{\infty}\sum_{n=1}^{\infty} \frac{m}{4} N_r I_n I_{n+m} L_m \sin(\theta_{n+m} - \theta_n) \\ & + \sum_{m=1}^{\infty}\sum_{n=1}^{\infty} \frac{2m+n}{4} N_r I_m I_{m+n} L_{n+2m} \sin(\theta_m + \theta_{n+2m}) \end{aligned} \quad (19)$$

Under this pattern of bipolar excitation, the average torque production is determined by the leading angle difference between the first and second order harmonics of phase current ahead of the self-inductance at the instant of aligned position of phase A. When the angle difference equals to 90° the maximum average torque will be produced under bipolar current excitation with alternate current components of at least two frequencies.

If the machine is excited by the current consisting of two different frequencies, it is quite complex to determine the saturation situation, which is not only related with the amplitude of alternate currents having two different frequencies, but also can be influenced by the leading angle difference between two alternate currents of different frequencies at the instant of aligned position of phase A. Therefore, if the magnitude of peak current is higher than I_s, the torque can be expressed as:

$$T = -\frac{1}{2}\left(\sum_{n=1}^{\infty} I_n \cos(nN_r\omega t + \theta_n)\right)^2 N_r \sum_{n=1}^{\infty} nL_n \sin(nN_r\theta) + \begin{pmatrix} \frac{1}{3}\left(\sum_{n=1}^{\infty} I_n \cos(nN_r\omega t + \theta_n)\right)^3 + \frac{1}{6} I_s^3 \\ -\frac{1}{2} I_s \left(\sum_{n=1}^{\infty} I_n \cos(nN_r\omega t + \theta_n)\right)^2 \end{pmatrix} \frac{dk_s}{d\theta} \quad (20)$$

C. Driven by Current of Two-Frequencies-II

An alternative method is to combine the former two bipolar excitation patterns together. In the single frequency method , it can be noticed that if the alternate current with frequency of $3/2N_r\omega$ is injected into the phase winding the overall torque

production will be increased since the overall torque due to the first order harmonic of self-inductance is not only produced by one single frequency $1/2N_r\omega$ but also produced by the alternate currents of two frequencies, viz. $1/2N_r\omega$ and $3/2N_r\omega$. In this case, the overall torque production can be considered as two major constitutions, one by the single frequency $1/2N_r\omega$ and the leading angle of $\theta_{1/2}$, another one by two frequencies $1/2N_r\omega$, $3/2N_r\omega$ and the leading angle difference of two frequencies at aligned position. It is worth to mention that alternate currents combined with more than one pattern of bipolar excitations can drive SRMs as well.

V. EXPERIMENT VERIFICATION

In order to verify the foregoing analyses and evaluate the accuracy of torque waveform and average torque prediction based on the Fourier series expression, the electromagnetic torque produced by the SRM under unipolar excitation, bipolar excitation of single frequency, bipolar excitation of two frequencies –I and II, respectively, the measurements are carried out on a prototype 6/4 SRM whose main parameters are given in Table I.

The measured torque waveforms in the following parts will be simply obtained from the interpolation of static torque corresponding to a given specific current and rotor position.

A. Unipolar Excitation

Fig.6 shows the phase current waveform and the corresponding FEA, measured and predicted results under unipolar excitation. The Fourier series expression is counted up to the 7th and 40th harmonics of self-inductance, respectively. It shows that counting up to the 7th harmonic of self-inductance is enough and only has small error with measurement.

B. Bipolar Excitation

Fig.7 shows the phase current, predicted and measured results under bipolar excitation of single frequency. It demonstrates the unidirectional torque production under bipolar excitation, and shows that the Fourier series model is able to calculate the torque under this excitation pattern. In Fig.7, it can also be noticed that although small negative torque is produced by a single phase, the resultant torque produced by all three phases is positive and unidirectional. This portion of small negative torque produced by one phase can contribute to reduce the torque ripple.

Fig.8 shows the phase current, predicted and measured results under bipolar excitation of two frequencies. It shows the torque production under this pattern of excitation is unidirectional, and the predicted results also have good agreement with measured results.

Fig.9 shows the phase current, predicted and measured results under bipolar excitations of both single frequency and two frequencies. Unlike the former two bipolar excitations the average torque production under this pattern of excitation is not only decided by the leading angle of $I_{1/2}$, but also determined by the leading angle difference between $I_{1/2}$ and $I_{3/2}$.

C. Average Torque and Torque Ripples

Fig.10 compares the average torque calculated by the proposed method under unipolar and all patterns of bipolar excitations. Fig.11 shows the average torque under the third pattern of bipolar excitation which is not only related to $\theta_{1/2}$, but also influenced by the leading angle difference between $\theta_{1/2}$ and $\theta_{3/2}$. Table II compares the maximum average torque, the corresponding torque ripple and RMS current under the same peak phase current, 10A. It should be noted that in order to ease the comparison under the same peak phase current, the unipolar current waveform is assumed to be composed of I_0 and I_1 only. It can be seen that at similar peak current the average torque under unipolar excitation and bipolar excitation with single frequency is similar. They are superior to that under bipolar excitation with two-frequencies I and II. However, the torque ripple under bipolar excitation with single frequency is smaller than that under unipolar excitation, and both are much lower than that under bipolar excitations with two-frequencies I and II. However, as shown in Table II, at maximum average torque production with the same peak current the RMS current values under the bipolar excitation with single frequency is highest and consequently lower $\overline{T}_{max}$ / RMS current than that of unipolar excitation.

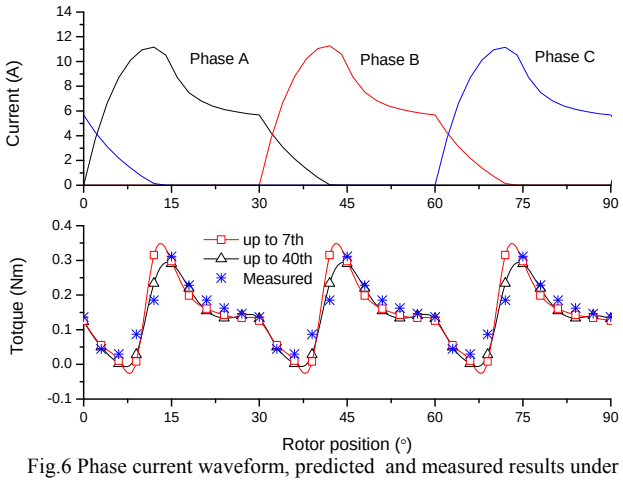

Fig.6 Phase current waveform, predicted and measured results under conventional unipolar excitation (advance angle=0°, Speed=1000rpm)

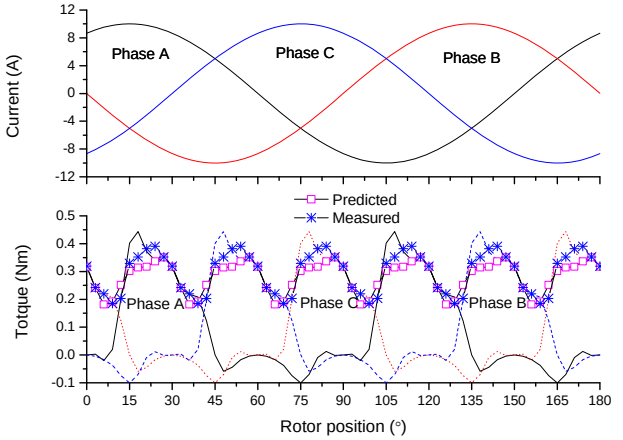

Fig.7 Phase current waveform, predicted (average torque=0.28Nm) and measured results (average torque=0.30Nm) under bipolar excitation of single frequency ($\theta_{1/2}$= 30°, $I_{1/2}$=10A)

VI. CONCLUSION

This paper derives the general analytical expression of average torque in SRMs under both unipolar and bipolar excitation, and to analyze their average torque under three working bipolar excitation patterns, with reference to unipolar excitation. All analyses are verified by the finite element analysis and measurements on a prototype 6/4 SRM.

It can be seen that at similar peak current the average torques under unipolar excitation and bipolar excitation with single frequency are similar, but the torque ripple under bipolar excitation with single frequency is smaller than that under unipolar excitation. However, both are better than other bipolar excitations with two frequencies in terms of torque and torque ripple.

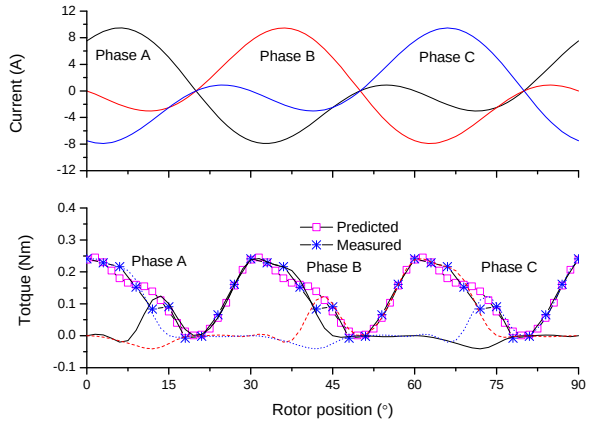

Fig.8 Phase current waveform, predicted (average torque=0.13Nm) and measured results (average torque=0.13Nm) under bipolar excitation of two frequencies (θ_1=0°, θ_3=60°, I_1=5A, I_2=5A)

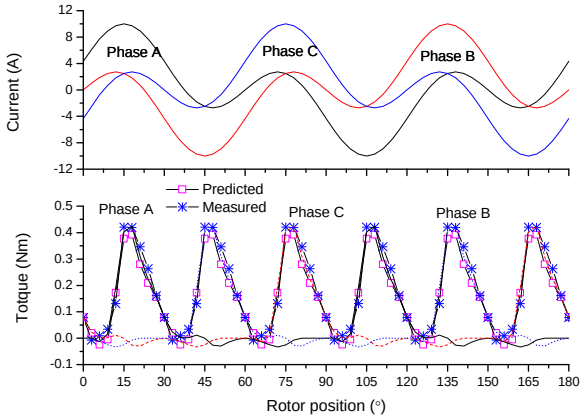

Fig.9 Phase current waveform, predicted (average torque=0.16Nm) and measured results (average torque=0.18Nm) under bipolar excitation of two frequencies ($\theta_{1/2}$=30°, $\theta_{3/2}$=90°, $I_{1/2}$=5A, $I_{3/2}$=5A)

TABLE I

COMPARISON OF MAXIMUM AVERAGE TORQUE, TORQUE RIPPLE, AND RMS CURRENT UNDER SAME PEAK CURRENT, 10A

Excitation pattern	1	2	3	4
$\overline{T}_{max}$ (Nm)	0.317	0.317	0.158	0.255
ΔT at $\overline{T}_{max}$ (Nm)	0.161	0.112	0.382	0.309
RMS current (A)	6.12	7.07	5.69	5.0
$\overline{T}_{max}$ / RMS current	0.0518	0.0448	0.0278	0.0510

1 – Unipolar (I_0=5A and I_1=5A); 2 - Bipolar with single frequency
3 - Bipolar with two frequencies-I; 4 - Bipolar with two frequencies-II

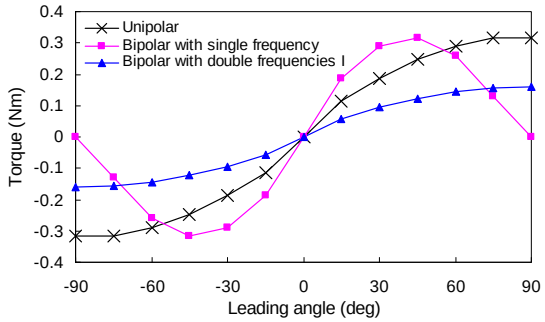

Fig. 10 Average torque comparison under unipolar and bipolar excitation with single frequency and two frequencies at the similar peak current (unipolar: I_0=5A, I_1=5A, bipolar with single frequency: $I_{1/2}$=10A, bipolar with double with double frequencies: I_1=5A, I_2=5A)

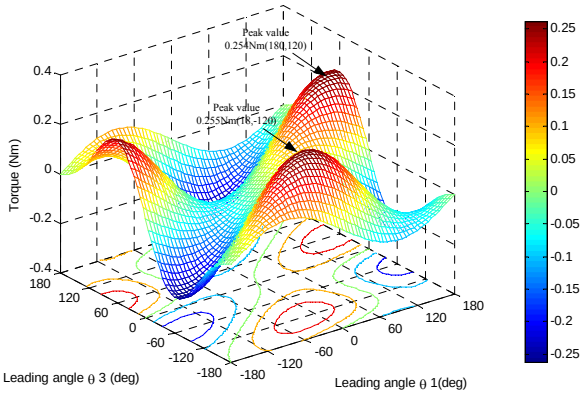

Fig. 11 Average torque under bipolar excitation with double frequencies II ($I_{1/2}$=5A, $I_{3/2}$=5A)

ACKNOWLEDGMENT

The authors thank JRI Solutions Ltd for providing JMAG software package.

REFERENCES

[1] Z.Q.Zhu, D.Howe, "Electric machines and drives for electric, hybrid, and fuel cell vehicles," *Proc. of IEEE*, vol.95, no.4, pp.746-765, 2007

[2] J.W.Ahn, S.G.Oh, J.W.Moon, and Y.M.Hwang, "A three-phase switched reluctance motor with two-phase excitation," *IEEE Trans. on Industry Appl.*, vol.35, no.5, Sep./Oct. 1999.

[3] C.S.Edrington, M.Krishnamurthy, and B.Fahimi, "Bipolar switched reluctance machines: a novel solution for automotive applications," *IEEE Trans.on Vehicular Tech.*, vol.54, no.3, pp.795-808, May 2005.

[4] P.J. Lawrenson, J.M.Stephenson, P.T.Blenkinsop, J.Corda, and N.N.Fulton, " Variable-speed switched reluctance motors," *IEE Proc.*, vol.127, no.4, pp.253-265, Jul. 1980.

[5] W. F. Ray, and R. M. Davis, "Inverter drive for doubly-salient reluctance motor: Its fundamental behavior, linear analysis and cost implications," *Inst. Elect. Eng. J. Elec. Power Applicat.*, vol. 2, no. 6, pp. 185–193, Dec. 1979.

[6] T.J.E.Miller, and M.McGilp, "Nonlinear theory of the switched reluctance motor for rapid computer-aided design," *IEE Proc.*, vol.137, no.6, pp.337-347, Nov.1990.

[7] D.A.Torrey, and J.H. Lang, "Modelling a nonlinear variable-reluctance motor drive," *IEE Proc. B. Electr. Power Appl.*, vol.137, no.5, pp.314-326, Sep.1990.

[8] S.J.Song, W.G.Liu, and Y.L.Wang, "Modeling, dynamic simulation and control of four-phase switched reluctance motor," *IEEE Int. Conf. on Control and Automation*, May/Jun. 2007, pp.1290-1295.

[9] P.Zaskalicky, and M.Zaskalicka, "Analytical method of calculation of current and torque of a reluctance stepper motor using Fourier complex-series," *Power Electronics and Motor Control Conference*, Sep. 2008, pp.899-902.